



TECHNICAL UNIVERSITY OF CLUJ-NAPOCA

ACTA TECHNICA NAPOCENSIS

Series: Applied Mathematics, Mechanics, and Engineering  
Vol. 66, Issue Special II, October, 2023

**PRECESSIONAL TRANSMISSIONS WITH MULTIPLE CONVEX-CONCAVE GEARS: STRUCTURAL SYNTHESIS, KINEMATICS AND CONTACT BEARING, GENERATION OF SURFACES**

**Ion BOSTAN**

***Abstract:** The article is dedicated to the research of precessional transmissions (PT) with multipair convex concave gears ( $A_{CX-CV}^D$ ). Aspects regarding the elaboration of precession gearing with multipair convex-concave tooth contact, the structural synthesis of the transmissions, the kinematics and tooth contact bearing are described. The influence of the geometric and kinematic parameters of the convex-concave gear on the relative sliding with friction between the mating flanks of the teeth and on the reduced curvature of the multipair mating flank profiles, and the bearing capacity and mechanical efficiency of the gear, respectively, is examined. The paper deals with technological procedures for generating non-standard tooth profiles by rolling with a spherospacial motion tool, as well as by generating them in the Gleason system on numerically controlled machine tools. Constructive-functional applications of kinematic and low-power precessional transmissions are described.*

***Key words:** precessional transmissions, load-bearing capacity, mechanical yield, convex-concave contact, generation of teeth by spatial rolling, the Gleason system on CNC machine tools.*

**1. INTRODUCTION**

The first invention „Precessional planetary transmission” with multiple gear with bolts  $A_{CX-CV}^B$  was registered on May 30, 1983 with the priority document date of 11.02.1982 SU 1020667 A, while the one with toothed gear  $A_{CX-CV}^D$  was registered on January 30, 1989 with the priority document date of 13.05.1986 (SU 1455094 A1).

Over the years precessional transmissions have been developed based on more than 30 kinematic structures of K-H-V and 2K-H types and their combinations 4K-2H and 6K-3H. The developed technical solutions have been protected by more than 200 invention patents and international patents, including 28 protected with the State Secret classified information „for official use”.

Figure 1 shows the kinematic structures of the 2K-H type precession transmissions and their combinations. Precessional transmissions can be gears with bolts with convex-concave tooth

contact  $A_{CX-CV}^B$ , with convex-rectilinear contact  $A_{CX-R}^B$  and with geared teeth with convex-rectilinear contact  $A_{CX-R}^D$ , with convex-concave contact with straight teeth  $A_{CX-CV}^D$  and convex-concave with inclined teeth or in circular arc  $A_{CX-CV}^{D,\beta}$ .

Transmission ratios of type 2K-H transmissions are determined by the relation (1).

$$i_{HV}^b = -\frac{Z_{g_1} \cdot Z_c}{Z_b \cdot Z_{g_2} - Z_{g_1} Z_c}, \tag{1}$$

where  $Z_b=Z_1, Z_{g_1}=Z_2, Z_{g_2}=Z_3, Z_c=Z_4$ , and those of 4K-2H transmissions – by the relation (2).

$$i_{HV_2}^b = -Z_{g_1} Z_c Z_{e_1} Z_d / Z_b Z_{g_2} (Z_b Z_{e_2} - Z_{e_1} Z_d) - Z_{g_1} Z_c (Z_b Z_{e_2} - Z_{e_1} Z_d), \tag{2}$$

The scientific research focused on the following development trends of precessional transmissions:

- The diversification of kinematic structures allowed to expand the range of transmission ratios of precessional transmissions, which have no analogues among the mechanical transmissions known worldwide.
- The development of the geometry of the multi-pair convex-concave contact with the small difference in the flank curves leads to the increase of the bearing capacity of the precessional transmissions.
- The gradual decrease of the relative sliding with friction between the teeth flanks leads to the increase of the mechanical efficiency of the precessional transmissions.

Precessional transmissions possess unique functional possibilities, including the actuating mechanisms of submersible machinery operated in conditions of hydrostatic pressure up to 70 MPa, also in conditions of absolute vacuum.

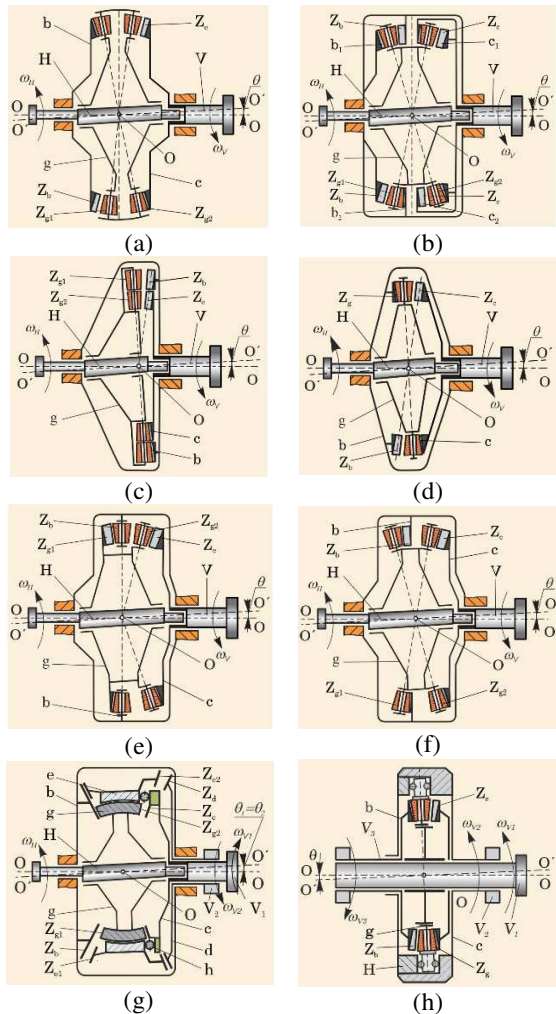


Fig.1. Kinematic 2K-H type structures

## 2. KINEMATICS OF PRECESSIONAL TRANSMISSIONS

The transmission ratio of the 2K-H type precessional transmissions, as well as the direction of rotation of the driving and driven shafts depend on the number of teeth of the geared wheels  $Z_1, 2, 3, 4$  and their correlation  $Z_{1(4)}=Z_{2(3)}\pm 1$ .

The following configurations of tooth number may be considered for 2K-H type of transmissions:

- I.  $Z_4=Z_3-1, Z_1=Z_2-1, Z_2=Z_3\pm 1, 2, 3, \dots$ , if for  $Z_2 > Z_3$  the driving and driven shafts rotate in different directions (fig. 2, a).
- II.  $Z_4=Z_3-1, Z_1=Z_2-1, Z_2=Z_3-1, 2, 3, \dots$ , if for  $Z_2 < Z_3$  the driving and driven shafts rotate in different directions (fig. 2, b).
- III.  $Z_4=Z_3+1, Z_1=Z_2-1, Z_2=Z_3-1, 2, 3, \dots$ , if  $Z_2 > Z_3$ , as well as for  $Z_2 < Z_3$  the driving and driven shafts rotate unidirectionally (fig. 2, c).
- IV.  $Z_4=Z_3-1, Z_1=Z_2+1, Z_2=Z_3\pm 1, 2, 3, \dots$ , if the driving and driven shafts rotate in different directions for both  $Z_2 > Z_3$ , as well as for  $Z_2 < Z_3$  (fig. 2, d).
- V.  $Z_4=Z_3+1, Z_1=Z_2+1, Z_2=Z_3+1, 2, 3, \dots$ , if  $Z_2 > Z_3$ , the driving and driven shafts rotate unidirectionally (fig. 2, e).
- VI.  $Z_4=Z_3+1, Z_1=Z_2+1, Z_2=Z_3-1, 2, 3, \dots$ , if  $Z_2 < Z_3$ , the driving and driven shafts rotate different directions (fig. 2, f).

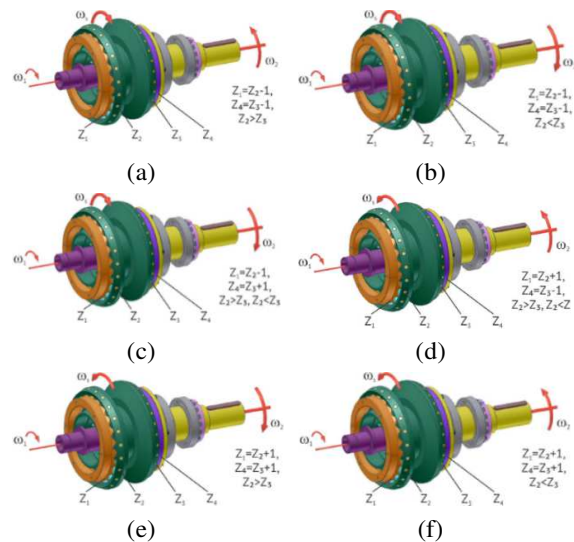


Fig.2. Precessional nodes with different correlation of the teeth number of the central wheels

### 3. CREATION OF PRECESSIONAL GEAR WITH MULTIPAIR CONVEX-CONCAVE CONTACT

In order to develop the convex-concave gear with spherospacial interaction of teeth expressed by the Euler kinematic equations, we admit the arbitrary description of the profile of the satellite-wheel teeth by a *LEM* circular arc of radius  $r$  with the center at point  $G$  (see fig. 3).

In the mobile coordinate system  $OX_1Y_1Z_1$ , rigidly linked to the satellite-wheel, the coordinates of the  $G$  center of the *LEM* circular arc of radius  $r$  are determined as follows:

$$X_{1G} = 0; Y_{1G} = -R \cos \delta; Z_{1G} = -R \sin \delta, \quad (3)$$

where  $\delta$  is the angle of the conical axoid.

Taking also into account (3) the relationship between the precession angles  $\psi$  of the crankshaft and self-rotation of the satellite-wheel  $\varphi$ ,  $\varphi = -\psi/Z_2$ , the authors determined the coordinates of the center  $G$  of the *LEM* circular arc of  $r$  radius depending on  $\psi$ :

$$\begin{aligned} X_G &= R \cos \delta \left[ -\cos \psi \sin \left( \frac{Z_1 \psi}{Z_2} \right) \right. \\ &+ \left. \sin \psi \cos \left( \frac{Z_1 \psi}{Z_2} \right) \cos \theta \right] - R \sin \delta \sin \theta \sin \psi; \\ Y_G &= -R \cos \delta \left[ \sin \psi \sin \left( \frac{Z_1 \psi}{Z_2} \right) \right. \\ &+ \left. \cos \psi \cos \left( \frac{Z_1 \psi}{Z_2} \right) \cos \theta \right] + R \sin \delta \sin \theta \sin \psi; \\ Z_G &= -R \cos \delta \cos \left( \frac{Z_1 \psi}{Z_2} \right) \sin \theta - R \cos \theta \sin \delta. \end{aligned} \quad (4)$$

Therefore, the center  $G$  of the circular arc *LEM* of radius  $r$ , which arbitrarily represents the flank profiles of the teeth of the satellite wheel, describes on the surface area of the radius  $R$  the trajectory  $\zeta_1=f(\zeta_1)$  defined by the coordinates  $X_G, Y_G, Z_G$  (fig. 3).

Using the rules of spherical trigonometry, the trajectory of the center  $G$  of the *LEM* circular arc expressed by  $\zeta_1=f(\zeta_1)$  is planned onto the plan  $P_1$ .

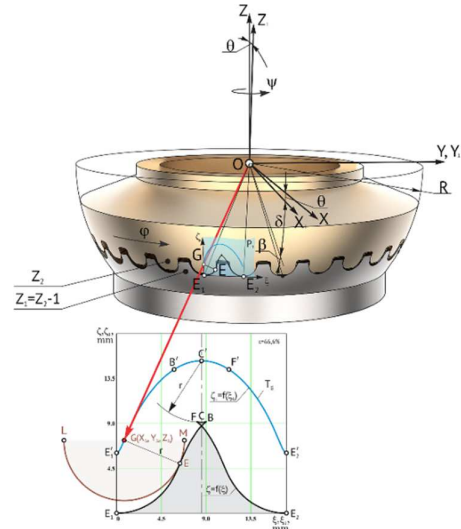


**Fig.3.** Motion projection of the center  $G$  of the curvature radius of *LEM* profile of the satellite-wheel teeth in normal section

Knowing the trajectory of the motion of the center of the circular arc *LEM* in the coordinates  $X_G, Y_G, Z_G$ , one may identify the position of the contact point  $E$  of the teeth of the satellite wheel and of the central wheel depending on the angular position  $\psi$  of the crankshaft.

The contact points  $E$  depending on the precession angle  $\psi$  are located at a distance  $r$  on the perpendicular line of the  $\mathbf{V}_G$  vector, the geometric totality of which within a precessional cycle  $0 \leq \psi \leq 2\pi Z_2/Z_1$  make up the profile of the central wheel teeth in the  $P_1$  plan.

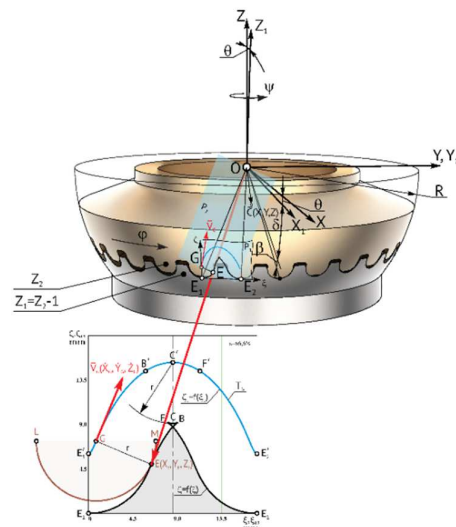


**Fig.4.** The tooth profile of the central wheels described by the  $G$  center velocity vector of the *LEM* profile of the satellite-wheel

In order to describe teeth profile of the central wheels, there may be identified the projections of the velocity vector  $\mathbf{V}_G$  on the axes of the mobile coordinate system  $OX_1Y_1Z_1$  (fig. 4).

For this, we derive equations (4) and identify a plan  $P_2$  – perpendicular to the velocity vector  $\mathbf{V}_G$ , which passes through the precession center  $O$  and the origin  $G_a$  of the circular arc  $LEM$ .

$$\begin{aligned}\dot{X}_G &= R\dot{\psi} \cos \delta \left[ \left(1 - \frac{Z_1}{Z_2} \cos \theta\right) \sin \psi \sin \left(\frac{Z_1\psi}{Z_2}\right) \right. \\ &+ \left. \left(\cos \theta - \frac{Z_1}{Z_2}\right) \cos \psi \cos \left(\frac{Z_1\psi}{Z_2}\right) \right] \\ &\quad - R\dot{\psi} \sin \theta \sin \delta \cos \psi; \\ \dot{Y}_G &= -R\dot{\psi} \cos \delta \left[ \left(1 - \frac{Z_1}{Z_2} \cos \theta\right) \cos \psi \sin \left(\frac{Z_1\psi}{Z_2}\right) \right. \\ &- \left. \left(\cos \theta - \frac{Z_1}{Z_2}\right) \sin \psi \cos \left(\frac{Z_1\psi}{Z_2}\right) \right] \\ &\quad - R\dot{\psi} \sin \theta \sin \delta \sin \psi; \\ \dot{Z}_G &= -R\dot{\psi} \left(\frac{Z_1}{Z_2}\right) \sin \theta \cos \delta \sin \left(\frac{Z_1\psi}{Z_2}\right).\end{aligned}\quad (5)$$

According to figure 4, the equation of the  $P_2$  plan is presented by the relation:

$$[\mathbf{OG} \times \mathbf{OC}] \times \mathbf{V}_G = 0. \quad (6)$$

Solving the vectorial product  $[\mathbf{OG} \times \mathbf{OC}]$  by opening on the elements of the first row results:

$$\begin{aligned}[\mathbf{OG} \times \mathbf{OC}] &= \begin{vmatrix} \mathbf{i} & \mathbf{j} & \mathbf{k} \\ X_G & Y_G & Z_G \\ X & Y & Z \end{vmatrix} = \mathbf{i}(Y_G Z - Z_G Y) \\ &+ \mathbf{j}(Z_G X - X_G Z) + \mathbf{k}(X_G Y - Y_G X),\end{aligned}\quad (7)$$

where  $X_G, Y_G, Z_G$  and  $X, Y, Z$  are the coordinates of the center  $G$  of the  $LEM$  profile of the circular arc satellite teeth and of an arbitrary point  $C$  on the  $P_2$  plan, respectively.

Using the expression (7) it was analogously described the vectorial equation  $[\mathbf{OG} \times \mathbf{OC}] \cdot \mathbf{V}_G = 0$  of the plan  $P_2$ , which results in:

$$\begin{vmatrix} i & j & k \\ Y_G Z - Z_G Y & Z_G X - X_G Z & X_G Y - Y_G X \\ \dot{X}_G & \dot{Y}_G & \dot{Z}_G \end{vmatrix} = 0, \quad (8)$$

and after matrix opening, we obtain the following equations:

$$\dot{Z}_G(XZ_G - ZX_G) - \dot{Y}_G(YX_G - XY_G) = 0; \quad (9)$$

$$\dot{X}_G(YX_G - XY_G) - \dot{Z}_G(ZY_G - YZ_G) = 0; \quad (10)$$

$$\dot{Y}_G(ZY_G - YZ_G) - \dot{X}_G(XZ_G - ZX_G) = 0. \quad (11)$$

The equation (11) results from (9) and (10) and can be adopted as equation of plan  $P_2$  in figure 4.

In order to identify the coordinates of the contact point  $E$  of the profiles of the satellite teeth and of the central wheel teeth, we consider that the point  $E$  belongs simultaneously to the plane  $P_2$  and the sphere with radius  $R$ . For these reasons, the coordinates of point  $E$  satisfy the equation of the plane  $P_2$ , for which reason we can write the equation:

$$(Z_G X_E - X_G Z_E) \dot{X}_G - (Y_G Z_E - Z_G Y_E) \dot{Y}_G = 0. \quad (12)$$

According to figure 4 the contact point of the teeth  $E$ , being on the sphere of radius  $R$  indicates that its coordinates satisfy the equation of this sphere.

$$X_E^2 + Y_E^2 + Z_E^2 - R^2 = 0, \quad (13)$$

while the angle between the vectors  $\mathbf{OG}$  and  $\mathbf{OE}$  constitutes the taper angle  $\beta$  of the satellite wheel teeth resulting in the following relation:

$$\mathbf{OG} \cdot \mathbf{OC} = R^2 \cos \beta \quad (14)$$

or

$$X_E Z_G + X_E Y_G + Z_E Z_G - R^2 \cos \beta = 0. \quad (15)$$

According to the equation (15) we obtain:

$$X_E = (R^2 \cos \beta - Y_E Y_G - Z_E Z_G) / X_G. \quad (16)$$

Substituting (16) in (12) we determine:

$$Y_E = k_1 Z_E - d_1, \quad (17)$$

and, respectively, (17) in (16), we obtain the expression of the  $X_E$  coordinate of the contact point  $E$ :

$$X_E = k_2 Z_E + d_2, \quad (18)$$

in which, after making some substitutions and transformations:

$$\begin{aligned}k_1 &= \frac{X_G \left( X_G \cdot \dot{X}_G + Y_G \dot{Y}_G \right) + Z_G^2 \dot{X}_G}{\left( X_G \dot{Y}_G - Y_G \dot{X}_G \right) Z_G}; \\ d_1 &= \frac{R^2 \cos \beta \dot{X}_G}{X_G \dot{Y}_G - Y_G \dot{X}_G}; \\ k_2 &= -\frac{k_1 Y_G + Z_G}{X_G}; \quad d_2 = \frac{R^2 \cos \beta + d_1 Y_G}{X_G}.\end{aligned}\quad (19)$$

By substituting (18) and (19) in (13) in relation to the  $Z_E$  coordinate of the contact point  $E$ , we obtain:

$$Z_E = (k_1 d_1 - k_2 d_2) \pm [(k_1 d_1 - k_2 d_2)^2 + (k_1^2 + k_2^2 + 1)(R^2 - d_1^2 - d_2^2)]^{1/2} / (k_1^2 + k_2^2 + 1). \quad (20)$$

According to figure 4, it can be concluded that the profile of the central wheel teeth is equidistant with the radius  $r$  of the motion trajectory of the center  $G$  of the circular arc  $LEM$ , and for any rotating angle  $\psi$  of the crankshaft the condition  $Z_E < Z_G$  should be met.

The relations (17), (18) and (20) represent the coordinates  $X_E$ ,  $Y_E$  and  $Z_E$  of the teeth contact point  $E$ , placed on the sphere.

Thus, the teeth profile on the sphere of radius  $R$  onto the plan  $P_1$  in two coordinates  $\xi$  and  $\zeta$  in the Cartesian system is projected according to the peculiarities of spherical trigonometry and can be determined according to the expressions:

$$\xi = \frac{[(E_1 E_2)^2 + v_1^2 - v_2^2]}{2(E_1 E_2)}; \quad \zeta = \sqrt{v_1^2 - \xi^2}. \quad (21)$$

where

$$(E_1 E_2)^2 = (X_{E_2} - X_{E_1})^2 + (Y_{E_2} - Y_{E_1})^2 + (Z_{E_2} - Z_{E_1})^2 = 0; \quad (22)$$

$$v_1^2 = (E_1 E_2)^2 = (X_N - X_{E_1})^2 + (Y_N - Y_{E_1})^2 + (Z_N - Z_{E_1})^2; \quad (23)$$

$$v_2^2 = (E_1 E_N)^2 = (X_N - X_{E_2})^2 + (Y_N - Y_{E_2})^2 + (Z_N - Z_{E_2})^2, \quad (24)$$

and the coordinates of the trajectory of the movement of the center  $G$  of the circular arc  $LEM$  of radius  $r$  by the expressions:

$$\xi_1 = \frac{[(E_1 E_2)^2 - S_1^2 - S_2^2]}{2(E_1 E_2)}; \quad \zeta_1 = \sqrt{S_1^2 - \xi_1^2}, \quad (25)$$

where

$$S_1^2 = (X_n - X_{E_1})^2 + (Y_n - Y_{E_1})^2 + (Z_n - Z_{E_1})^2; \quad (26)$$

$$S_2^2 = (X_n - X_{E_2})^2 + (Y_n - Y_{E_2})^2 + (Z_n - Z_{E_2})^2; \quad (27)$$

$$(E_1 E_2)^2 = (X_{E_2} - X_{E_1})^2 + (Y_{E_2} - Y_{E_1})^2 + (Z_{E_2} - Z_{E_1})^2 = 0. \quad (28)$$

The expressions (25) represent the coordinates of the projection of the trajectory of the movement of the centers  $G$  of the  $LEM$  circular arcs on the  $P_1$  plan, and the expressions (21) represent the coordinates of the profile of the central wheel teeth projected on the  $P_1$  plan.

#### 4. KINEMATICS AND GEOMETRY OF THE TEETH CONTACT

According to the fundamental theory of precessional gears with toothed gearing [2, 4], depending on the shape of the tooth profiles and the pressure angle between the flanks  $\alpha_w$ , they can operate in reducer, multiplier and differential mode.

Figure 5 shows the precessional node of the 2K-H type gear with the parametric configuration for the reducer operating regime, with the transmission ratio  $i = -124$ , and figure 5 (b) – with the parametric configuration for the multiplier, operating regime, with the multiplication ratio  $i=14,09$ . In the gear figure 5 (b), the multiplier operating regime is ensured by the gearing  $(Z_1-Z_2)$  with the ratio of the teeth numbers  $Z_1=Z_2+1$ , where the profile angle of the central wheel teeth  $\alpha > 45^\circ$ . When the driving shaft of the multiplier rotates with angular velocity  $\omega_1$ , the teeth of the central wheel with the angle of the profile of the teeth  $\alpha > 45^\circ$  transform the rotational motion of the satellite teeth with  $Z_2$  into spherospacial motion of the satellite wheel, gearing its teeth  $Z_3$  with the teeth  $Z_4$  of the mobile central wheel.

In the toothed precessional gear (fig. 5), by changing the shape of the central wheel tooth, the multiplicity of the gearing reduced from 100% pairs of teeth simultaneously geared to 26,6% pairs, or 13,3% pairs of teeth with contact on the active profile of the central wheel teeth.

Thus, the contacts of the flanks with relatively high sliding were excluded from the gearing, being created favorable conditions for varying the parametric configuration  $[Z_g - \theta, \pm 1]$  regarding the creation of the convex-concave contact geometry with little difference in the radii of curvature of the conjugated profiles.

#### 5. INFLUENCE OF GEAR PARAMETERS ON GEOMETRY AND KINEMATICS OF CONTACT

Based on the analysis of the functions  $\zeta=f(\xi)$  and  $\zeta_1=f(\xi_1)$  described by the equations (21) and (22), and of the kinematics of the contact point of the teeth in the multiple gear  $A_{CX-CV}^D$  it was found out that the angles of nutation  $\theta$ , of the



conical axoid  $\delta$  and the angles of conicity of the satellite wheel teeth  $\beta$ , the number of teeth  $Z_{1,2,3,4}$  and their ratio gradually and vectorially influence the flank curves  $\rho_{k_i}$  of the teeth and the difference of the curves ( $\rho_{k_i} - r$ ).

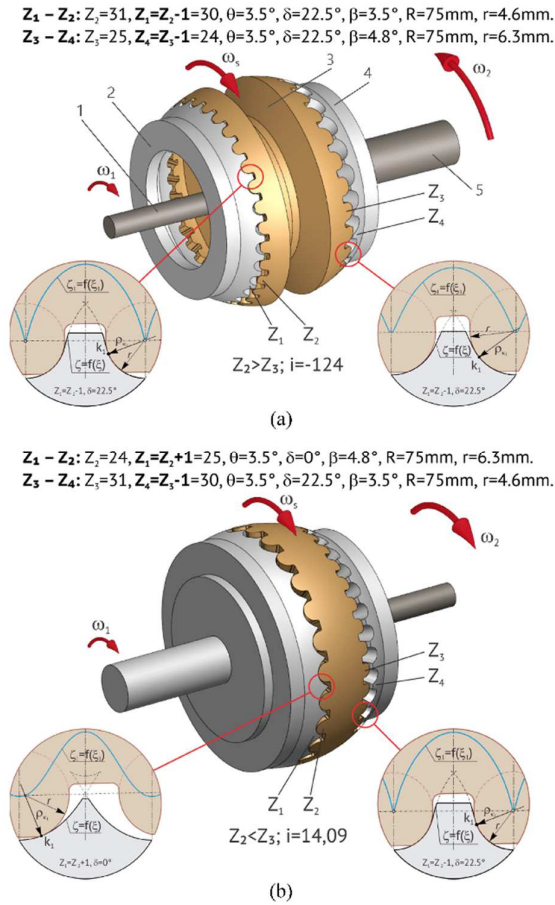


**Fig.5.** The teeth profiles of the crowns of gearings ( $Z_1 - Z_2$ ) and ( $Z_3 - Z_4$ ) in the precessional gear with reducer (a) and multiplier (b) regimes: 1 - crank shaft, 2 - fixed central wheel, 3- satellite wheel, 4 - movable central wheel, 5- driven shaft

It was also established that the parameters  $\theta$ ,  $\delta$ ,  $\beta$ ,  $Z_{1,2,3,4}$  and their correlation  $Z_{1(4)}=Z_{2(3)}\pm 1$  influence the relative sliding speed with friction  $V_{al}$  between the teeth simultaneously conjugated to one and the same angular coordinate  $\psi$  of the crankshaft. These parameters constitute the parametric configuration  $[Z_g - \theta, \pm 1]$ , which defines the influence of each constituent parameter individually and as a whole.

Figure 6 shows a range of profilograms of the flank profiles and of the contacts of the teeth

simultaneously conjugated to one and the same positioning of the crankshaft  $\psi$  for different value correlation of the configuration parameters  $[Z_g - \theta, \pm 1]$ .

Figure 6 shows examples of tooth profiles modified according to the dispersion of the contact points  $k_i$  of the simultaneously conjugated flanks in the gears  $A_{CX-CV}^D$  with the correlation  $Z_1=Z_2-1$ . In the presented profilograms, the functions  $\zeta^*=f(\zeta^*)$  and  $\zeta_1^*=f(\zeta_1^*)$  represent, respectively, the trajectory of the motion of the origin of the circle arc  $G$  of the profile of the satellite wheel teeth and the profile of the central wheel teeth, expressed in parametric form in Cartesian coordinates, with the variation of the precession angle from  $\psi=0^\circ$  to  $\psi=2\pi Z_2/Z_1$ .

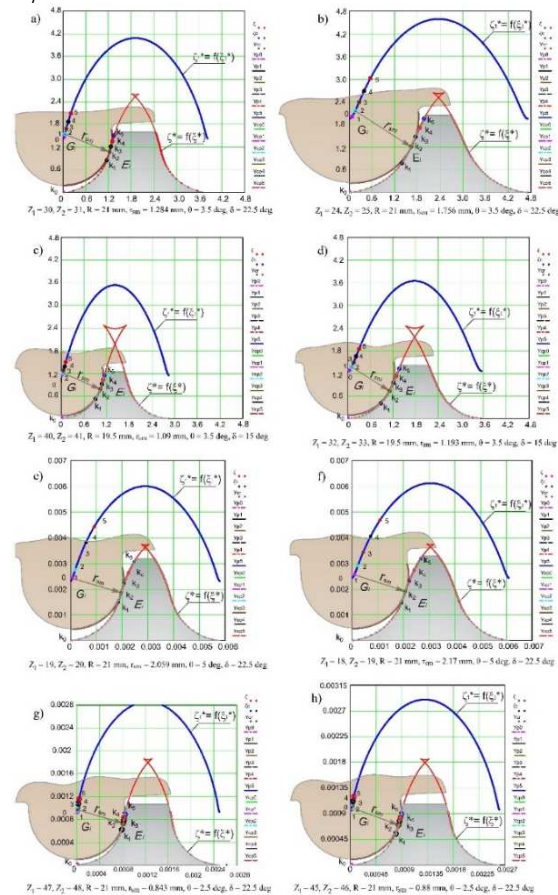


**Fig.6.** Flank profiles modified according to the dispersion of the contact points  $k_i$  of the conjugated teeth simultaneously in the precessional gearing  $A_{CX-CV}^D$  with  $Z_1=Z_2-1$

The profiles presented in figure 6 are recommended for the elaboration of

precessional transmissions with reducer operation regime and with transmission ratio in the range  $\pm 20 \leq i \leq \pm 3600$  where the number of teeth  $Z_{1,2,3,4} \leq 60$ . The contact points  $k_0 \dots k_i$  of the flanks of the teeth in the gear area are transposed on the profile of the teeth of the central wheels according to  $\psi$ , corresponding to each of the pairs of teeth simultaneously conjugated.

## 6. MODIFICATION OF TEETH PROFILES

The modification of the profiles of the conjugated teeth in the precessional gears  $A_{CX-CV}^D$  consists in the exclusion from the gear of the pairs of teeth in contacts with convex-convex and/or convex-rectilinear geometry, also in which the relative sliding between flanks is large. As a result, by excluding these pairs of teeth from the gear area, on the one hand it ensures the reduction of the relative sliding friction between the flank profiles of the teeth, and on the other hand it ensures the prevalence of the contacts with convex-concave geometry of the conjugated flanks with small curvature difference. At the same time, by modifying the tips of the satellite wheel teeth with a circle arc profile, the phenomenon of tooth gearing with "head to foot" blows is excluded, and by profiling the teeth tip with a radius of curvature  $r_a > r$  the creation of the contact geometry favorable to lubrication and the existence of low-friction lubrication regimes between the flanks is ensured.

In the gear  $A_{CX-CV}^D$  with  $Z_1=32, Z_2=33, \theta=3,5^\circ$  and  $\delta_{(1-2)}=22,5^\circ$  with modified profiles (fig. 7, a), with the rotation of the crankshaft, the flanks of one and the same pair of teeth contacts consecutively in the contacts  $k_0 \dots k_i$  with the angular coordinates  $\psi_{k_i} = 2\pi Z_1 / Z_1^2 \cdot i$ , where  $i=0, 1, 2 \dots$  is the order number of the tooth contact corresponding to the rotation of the crankshaft with the angular pitch  $\psi_k$ .

That if the precession angle  $\psi=0^\circ$  the mechanism of transforming the rotational motion of the crankshaft into spherospacial motion of the satellite wheel ensures the contact of the tip of the satellite wheel tooth in a circle arc with the foot of the central wheel tooth at the point  $k_0$  located at the boundary between the

passive and active profiles of the central wheel tooth.

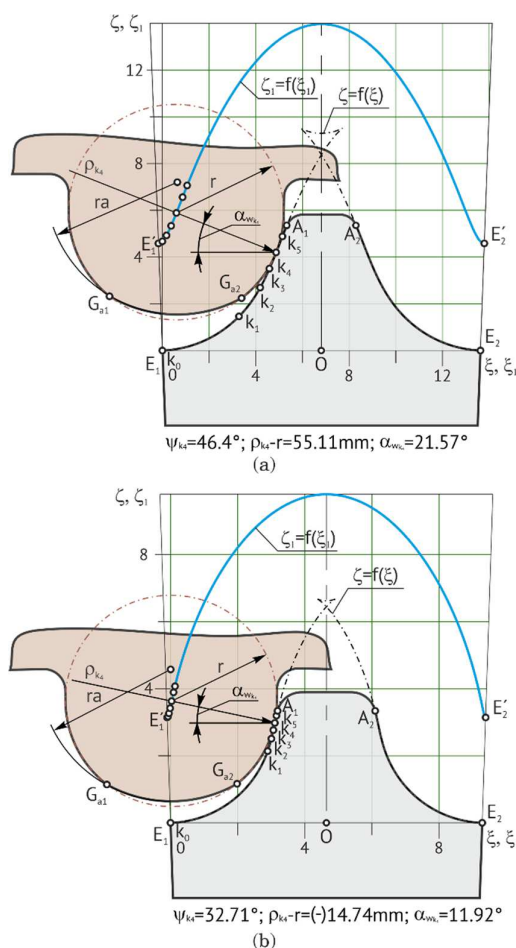


**Fig.7.** Dispersion of the contact points  $k_i$  and the pressure angle  $\alpha_w$  between the flanks of the conjugated teeth in the gears  $A_{CX-CV}^D$ : a)  $Z_1=32, Z_2=33, R_m=75 \text{ mm}, r=4,58 \text{ mm}, \theta=3,5^\circ, \delta=15^\circ, \beta=3,5^\circ$ ; b)  $Z_1=45, Z_2=46, R_m=75 \text{ mm}, r=3,14 \text{ mm}, \theta=2,5^\circ, \delta=22,5^\circ, \beta=2,4^\circ$

When rotating the crankshaft at an angle between two adjacent teeth of the central wheel, i.e. with the angular pitch  $\psi_k = 2\pi Z_1 / Z_1^2$ , the flanks of the teeth of the same pair of teeth will contact at the next contact point  $k_1$ .

When rotating the crankshaft 1 (fig. 5) with two angular steps, i.e. with  $\psi_k = 720^\circ Z_1 / Z_1^2$ , the flanks of the teeth of the same pair of teeth will contact at the contact point  $k_2$  and so on. We admit that in the profilograms (fig. 7 a, b), depending on the shortening of the height of the teeth, in the gear area simultaneously contact four pairs of teeth required with load.

The evolution of the succession of the gearing of the teeth simultaneously conjugated in the contacts  $k_0, k_1 \dots k_i$  and their geometric dispersion are presented in figure 7.

In case of gearing  $A_{CX-CV}^D$  with  $Z_1=24, Z_2=25, \beta_3=4,78^\circ, \theta=3,5^\circ, \delta_{(1-2)}=22,5^\circ, R_m=21 \text{ mm}, r_{sm}=1,76 \text{ mm}$ ; the evolution of the conjugation of the teeth is presented in the conventional unfolding (see fig. 8, a).

The contact points of the teeth  $k_0, k_1, k_4$  have the angular coordinates expressed by the precession angle, respectively  $\psi_{k_0}=0^\circ, \psi_{k_1}=15,62^\circ, \psi_{k_2}=31,25^\circ, \psi_{k_3}=46,87^\circ$  and  $\psi_{k_4}=62,49^\circ$ . Also, the dispersion of the contact points  $k_0, k_1 \dots k_4$  of the teeth simultaneously conjugated at one and the same positioning of the conventional crankshaft transposed on the active profile of the central wheel tooth is shown in figure 8 (b).

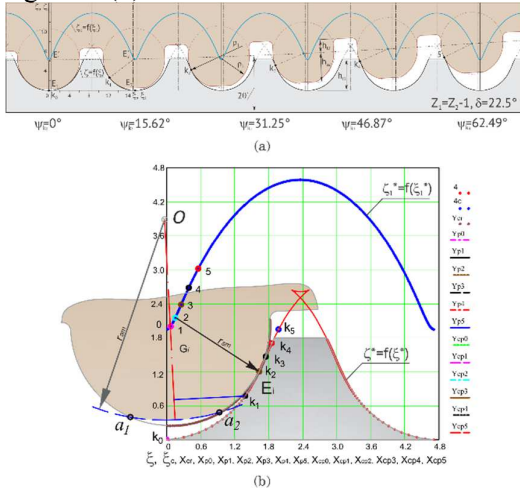


**Fig.8.** The multiple pair contact of the conjugated teeth simultaneously in the gear  $A_{CX-CV}^D$  in unfolding:  $Z_1=24, Z_2=25, R_m=21 \text{ mm}, r_{sm}=1,76 \text{ mm}, \theta=3,5^\circ, \delta_{(1-2)}=22,5^\circ, \beta=3,5^\circ$

The profile of the teeth of the central wheels is modified by shortening their height, so that the contact  $k_5$  of the teeth with the coordinate  $\psi_{k_5}=78,11^\circ$  is placed outside the gear area of the teeth. The tips of the satellite wheel teeth are modified by profiling according to figure 8 (b), so that the contact of the satellite wheel teeth for the angular coordinate  $\psi_{k_0}=0^\circ$  to rest on the profile of the central wheel at points  $a_1$  and  $a_2$ , geometrically dependent on the size of the radius

of the circle arc  $r_{am}$  and on the correlation  $r_{sm}/r_{am}$ . If the semi-arcs  $\cup a_1 a_2 / 2 = \cup k_0 k_1$ , the teeth will not contact each other along the length of the arc  $k_0 k_1$ , so a pair of teeth is completely excluded from gear area, and if the tips of the satellite wheel teeth are described by the semi-arc  $\cup a_1 a_2 / 2 < \cup k_0 k_1$ , only part of a pair of teeth, proportional to the correlation of the arc  $\cup a_1 a_2 / 2$  and  $\cup k_0 k_1$  is excluded from the gear.

In the images in figure 7 it is observed that for one and the same angular positioning of the crankshaft, a certain number of pairs of teeth defined by the degree of modification of the teeth by shortening their height are conjugated simultaneously in the gear. At the same time, it is found that the dispersion of the contact points  $k_0 \dots k_4$  of the teeth simultaneously conjugated from the gears  $A_{CX-CV}^D$  with different parameters of the configuration  $[Z_g - \theta, \pm 1]$  is different.

The dispersion of the contact points of the teeth simultaneously conjugated  $k_i$  to one and the same angular positioning of the crankshaft in the gear with the parametric configuration  $[Z_g - \theta, \pm 1]$ , shown in figure 7 (a), is higher than in the gear shown in figure 7 (b) and, respectively, decreases the average value of the pressure angles  $\alpha_w$  between the flanks of the simultaneously conjugated teeth.

Figure 8 (a) shows the topographic interpretation of the ongoing evolution of the gearing sequence of the flank profiles of the teeth simultaneously conjugated at the points  $k_0, k_1 \dots k_i$  at one and the same angular positioning of the crankshaft  $\psi_k$ , and in figure 8 (b) is shown the dispersion of the contacts  $k_i$  conventionally transposed on the active profile of the teeth of the central wheel, also for one and the same positioning of the crankshaft  $\psi_{k_i}$ .

From the analysis of the evolution of the positioning of the contact points of the flanks of the teeth  $k_1 \dots k_4$  and of their dispersion, we find that the rotation angles of the crankshaft at which the contact points of the flanks migrate from the contact  $k_1$  to the contact  $k_4$  are different for the same number of pairs of teeth simultaneously conjugated. Also, from figure 7 it results that the pressure angle between the flanks is smaller in the gear from figure 7 (b), in which the dispersion of the contact points  $k_i$  is



smaller, and vice versa, the pressure angle between the flanks increases in the gearing in figure 7 (a) as the dispersion of the contact points of the conjugated flanks increases.

Procedurally, the geometric shape of the teeth is modified by shortening and cutting their tips in correlation with the dispersion of the contact points  $k_0...k_i$  of the flanks simultaneously conjugated in the gears  $A_{CX-CV}^D$  with concrete configuration parameters  $[Z_g - \theta, \pm 1]$ .

In this context it is important to analyze the topology of the dispersion of the contact points  $k_i$  of the simultaneously conjugated teeth according to the configuration parameters  $[Z_g - \theta, \pm 1]$  which define both the shape of the tooth profiles and the convex-concave geometry of the contacts  $k_i$  of the conjugated.

From the comparative analysis of the profilograms of the conjugated teeth from the gears  $A_{CX-CV}^D$  with the correlation of the tooth numbers  $Z_1=Z_2-1$  and the concrete parameters of the configuration  $[Z_g-\theta,-1]$ . (see fig. 6) it is attested that the dispersion of the contact points  $k_0...k_i$  of the conjugated profiles decreases with the increase of the angle of the conical axoid  $\delta_{(1-2)}$  and practically does not depend on the nutation angle  $\theta$  the radius of the circle arc  $r$  of the profiles of the satellite wheel teeth and the number of teeth  $Z_1$  of the central wheel.

The dispersion of the contact points  $k_0...k_i$  transposed on the profile of the tooth of the central wheel topologically is defined by their angular coordinates, expressed by the precession angle  $\psi$ , determined from  $\psi_{k_i} = 2\pi Z_2 i / Z_1^2$ , where  $i=0, 1, 2...5$  is the order number of the contact noted starting with  $k_0$ .

Figure 9 shows the evolution of the positioning of the circle arc profiles of the multiple pair conjugated satellite wheel teeth with the convex-concave profiles of the central wheel teeth for one and the same position of the crankshaft  $\psi$  in the gears  $A_{CX-CV}^D$  with: (a)  $Z_1=32$ ,  $Z_2=33$ ,  $R=75 \text{ mm}$ ,  $r=4,58 \text{ mm}$ ,  $\theta=3,5^\circ$ ,  $\delta=15^\circ$ ,  $\beta=3,5^\circ$ ; (b)  $Z_1=45$ ,  $Z_2=46$ ,  $R=75 \text{ mm}$ ,  $r=3,14 \text{ mm}$ ,  $\theta=2,5^\circ$ ,  $\delta=22,5^\circ$ ,  $\beta=2,4^\circ$ .

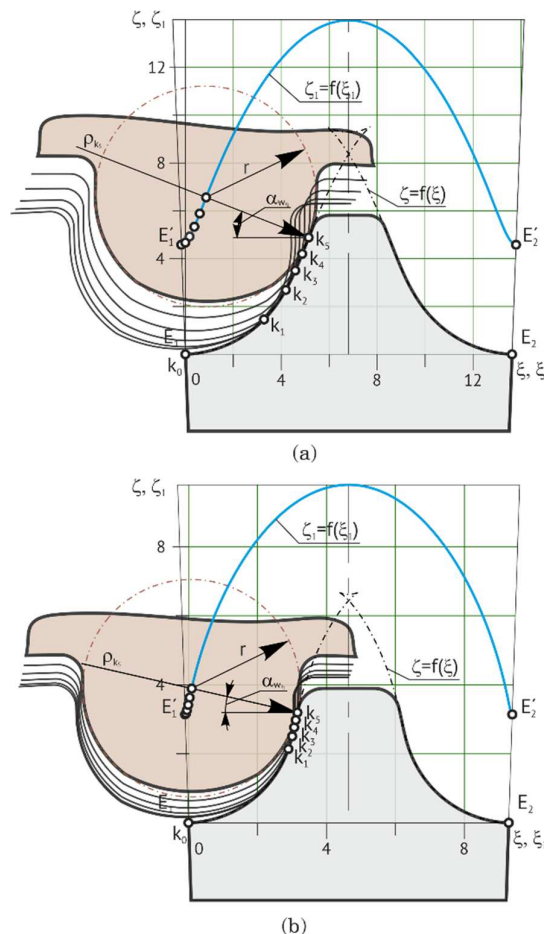


**Fig.9.** The sequence of positioning the profiles of the multiple pair conjugated teeth in the contacts  $k_0...k_5$  at one and the same angular coordinate  $\psi$  of the crankshaft in the gears  $A_{CX-CV}^D$

When the crankshaft 1 (fig. 5) is rotated continuously at angular velocity  $\omega_1=f(\psi)$ , the circle arc teeth of the satellite wheel are conjugated multiparously with the teeth of the central wheels with convex-concave profiles in the contacts  $k_i$ , passing successively from one tooth to another, if the crankshaft rotates at an angle equal to the angular pitch  $\psi_k = 360Z_2/Z_1^2$  between two contacts of the pairs of neighboring teeth.

From the analysis of the specificity of tooth conjugation in the precessional gear  $A_{CX-CV}^D$  and in the Wildhaber-Novikov gear, it is found that: gear consists in the fact that in both gears the teeth are conjugated in contacts with convex-concave geometries with the same (comparable) small difference of the radii of curvature of the conjugated flanks, at the same time the

peculiarities of precessional gearing consist in the simultaneous multipair conjugation of the teeth under load, which constitute three to five times more pairs of teeth.

Therefore, it is found that the precessional transmissions with  $A_{CX-CV}^D$  gears, compared to the Wildhaber – Novikov (W-N) transmissions, from the point of view of the deformable contact mechanics and the multiple pair contact conditions are more efficient, because both gears having contacts between teeth with convex-concave geometries with the same (comparable) small difference of the flank curves, in W-N transmissions, in the frontal gear are conjugated only up to a pair of teeth, and in the precessional one – up to three to five pairs of teeth.

In accordance with the above, in the approaches to the development of precessional transmissions with gears  $A_{CX-CV}^D$  and in the comparative analyzes of the contact bearing and of the multiple pair contact conditions, we are to take into account the following finding:

*In precessional transmissions with the gear  $A_{CX-CV}^D$  and in Wildhaber-Novikov transmissions the teeth are conjugated in contacts with convex-concave geometries with the same (comparable) small difference in flank curves, which from the point of view of the mechanics of the deformable solid defines the bearing contact of the teeth, but at the same time, in precessional transmissions, the number of pairs of teeth simultaneously conjugated under load is up to 3-5 times higher than in W-N transmissions [8].*

## 7. GENERATION OF TEETH WITH A CONVEX/CONCAVE PROFILE THROUGH ROLLING-SPACE ROLLING WITH A “TRUNK OF CONE” TOOL

The teeth profile of the central wheels of the precessional gear is variable depending on the values of the geometric parameters of the configuration [ $Z_g - \theta, \pm 1$ ].

For these reasons, a new procedure was proposed for generating the central wheel teeth by spatial tumbling-rolling notified by  $G_{F.S}^{con}$ , which ensures the realization of a lot of profiles of the teeth, using a tool with the same geometric parameters [4].

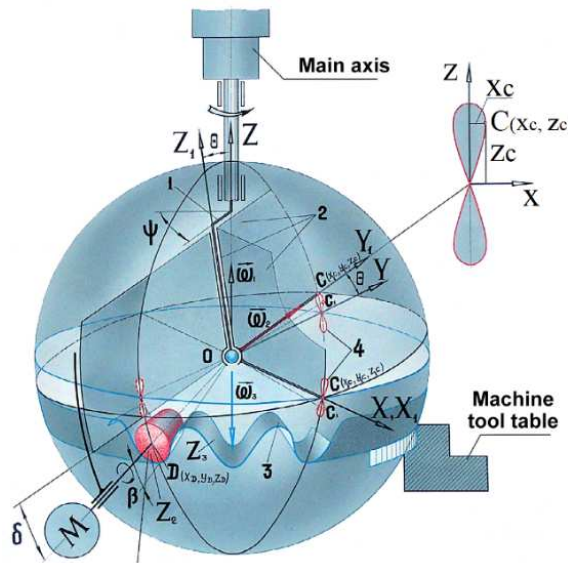


**Fig.10.** The conceptual spatial scheme of the teeth generating process by spatial tumbling-rolling (with precessional tool) [4]

The process for generating of variable profiles, was based on the constructive-kinematic concept of the tool holder mechanism, reproducing the contact geometry and the interaction with spherospacial motion of conjugated teeth in real precessional transmission (fig. 10) [3, 4].

In the elaborated mechanism, the node that engages the tool in the shape of “cone trunk”, in spherospacial motion 2 through a kinematic link joint 4 is stopped from rotating around the common axis  $OZ$  of the *main shaft of the machine tool-blank* and of the blank.

The (neasuric) kinematic link joint 4 of the tool with the machine tool rod must be constructed so as to ensure the continuity of the rotational motion transformation function, so  $\omega_1/\omega_3=\text{const}$ . We analyze the continuity of the rotational motion transformation function through the motion trajectory of the point  $C$ , which belongs to the mobile coordinate system.

In figure 11 are presented the profilograms of the generation of the teeth profile. On the profilograms, the curve 1 represents the motion trajectory of the tool center in the immobile coordinate system  $OXYZ$ , and the curve 2 – the motion trajectory of the tool center in the mobile coordinate system  $O\bar{X}\bar{Y}\bar{Z}$ , the curve 3 shows the

wrap of the precessional tool surfaces family (tooth profile), the curve 4 – the contour of the profile generating tool. Analyzing the profilograms (fig. 11) it is demonstrated the degree and character of the influence of the tool location angle  $\delta$  with respect to the plane  $OX_1Y_1$ , of the radius of the tool  $R$  and of the transmission ratio  $i$  of the *main shaft-blank* kinematic chain on the shape of the central wheel teeth profile.

For the manufacture of the variable convex/concave flank profiles of the teeth of the central conical wheels (fig. 12), the process of generating the teeth by spatial tumbling-rolling with the tool of the "cone trunk" shape was developed, notified by  $G_{r,s}^{con}$ .

Figure 12 shows the main scheme of the process  $G_{r,s}^{con}$  for generating tooth flanks with variable shape protected by the patent SU 1563319 A1 (ДСП)\*, authors I. Bostan and I. Babaian.

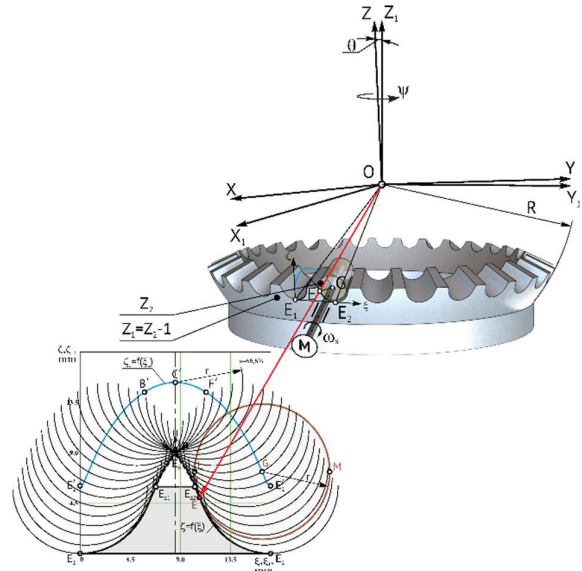


**Fig.12.** The scheme of the process of generating the teeth with variable convex/concave profiles with the tool of the "cone trunk" shape

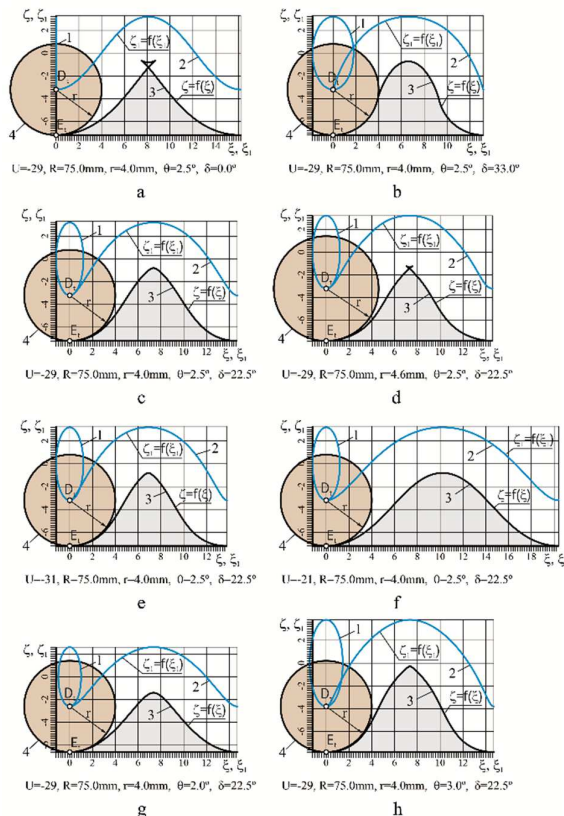


**Fig.11.** Profilograms of the generating process  $G_{r,s}^{con}$  of the teeth profile with the precessional tool in the shape of a "cone trunk"

Currently, in modern industry, wheels with conical teeth can mainly be made according to four different systems, characterized by the shape of the guiding curve of the tooth flanks:

1. In the Oerlikon-Elloid system, the conical toothing has the guiding curve of the tooth flanks in the shape of an elongated epicycloid arc and is made on toothing machine tools manufactured by the *Oerlikon-Geatrec* Company from Switzerland.
2. The Klingelberg-Ziklo-Polloid toothing system is characterized by the guiding curve of the flanks of the teeth, also by the shape of the elongated epicycloid, but the knife holder head consists of two overlapping parts, on which the knives corresponding to the convex and concave flanks are arranged separately. The toothing machine tools of this toothing system are made by the Klingelberg Company in Huckeswagen, Germany.
3. In the Klingelberg-Ziklo-Polloid toothing system, the guiding curve of the tooth flanks is an elongated involute, and the profile generating tool is a cone-shaped auger cutter. The respective machine tools are produced at the same Klingelberg Company in Huckeswagen, Germany.

\*State Secret classified information „for official use”.



4. In the Gleason tothing system, the guiding curve of the tooth flanks is a circle arc and is made on tothing machine tools manufactured by the *Gleason Works Company* in Rochester, N.I., USA.

The precessional gears  $A_{CX-CV}^{D,\beta}$  with curvilinear teeth are defined by the specific peculiarities of the convex-concave profiles of the teeth with spherospacial interaction, including the topography of the contact lines of multiple-pair conjugated curvilinear teeth.

The tooth profiles of of the wheels of precessional gears with inclined teeth  $A_{CX-CV}^{D,\beta}$ , analogous to those of gears with straight teeth  $A_{CX-CV}^D$ , can be executed according to of the equations  $\zeta=f(\xi)$  on numerically controlled machine tools (CNC) [8].

The manufacture of wheels with precessional gearing  $A_{CX-CV}^{D,\beta}$  was carried out in cooperation with the Gleason Corporation, USA based on an agreement signed with the Technical University of Moldova.

The mobile and immobile central wheels, including the teeth of the satellite wheel, were made of carbon steel 4140 and plastic material PEEK (Poly Ether Ether Ketone) Glass-Filled with 30% glass fiber. The toothed wheels, depending on the transmitted load and the operating regime, can be assembled in transmissions so that the conjugated teeth form the tribological couples *plastic-plastic*, *steel-plastic* and *steel-steel*.

Figure 13 (h) shows the general view of the 2K-H precessional transmission with the transmission ratio  $i=-45$  with gears  $A_{CX-CV}^D$  with configuration parameters  $[Z_g, -\theta, -1]$ :  $Z_1=44$ ,  $Z_2=45$ ,  $\delta_{(1-2)}=15^\circ$ ,  $\beta_2=2,4^\circ$ ,  $Z_3=23$ ,  $Z_4=22$ ,  $\delta_{(3-4)}=22,5^\circ$ ,  $\beta_3=4,7^\circ$ ,  $\theta=3,5^\circ$  and  $D_e=42$  mm).

In the figure 13 (b), (c) the profilograms of the teeth ( $Z_1-Z_2$ ) and ( $Z_3-Z_4$ ) are shown, respectively, in (e) – the central wheels and the satellite wheel unfolded, manufactured on CNC machine tools from materials in the couples: *steel-plastic*, *plastic-steel*, *steel-steel* and *plastic-plastic*.

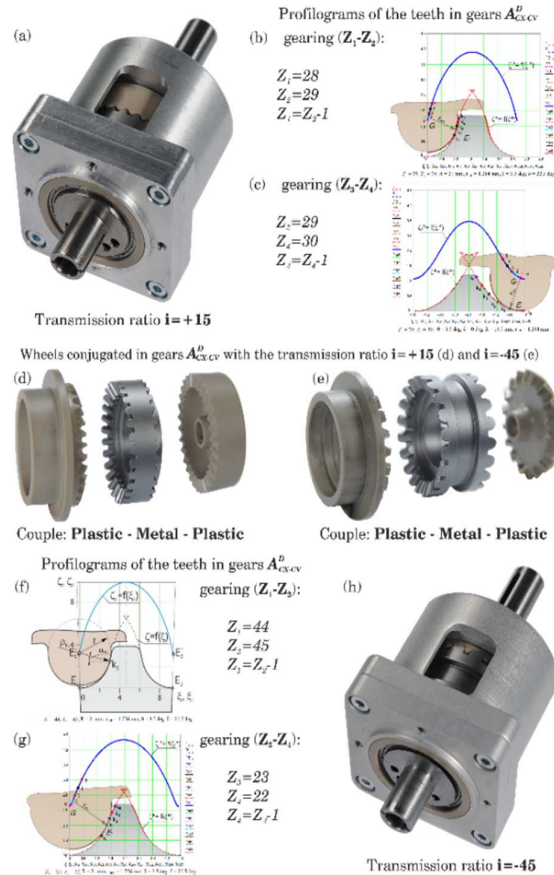


**Fig.13.** 2K-H kinematic precessional transmissions, with  $i= + 15$  (a), achieved in the gears  $A_{CX-CV}^D$  (b) and (c), and with the transmission ratio  $i= - 45$  (h), achieved in the gears  $A_{CX-CV}^D$  (f) and (g), with toothed wheels (d) and (e) manufactured on CNC machine tools

Figure 14 (a) shows the fabricated sample of the 2K-H ( $i=-75$ ) precessional transmission with gearings  $A_{CX-CV}^{D,\beta}$  with circle arc toothings and satellite-wheel mounted axially floating on the crankshaft with concurrent axes in the precession center.

Figure 14 (b) shows samples of central wheels 1 and 3 and satellite-wheel 2 fabricated from 4140 steel on numerically controlled multi-axis machine tools in cooperation with *Gleason Corporation*, USA, and figure 14 (c) – the original components of the 2K-H precessional transmission with gearings  $A_{CX-CV}^{D,\beta}$  with the transmission ratio ( $i=-75$ ) in progress unfolding.



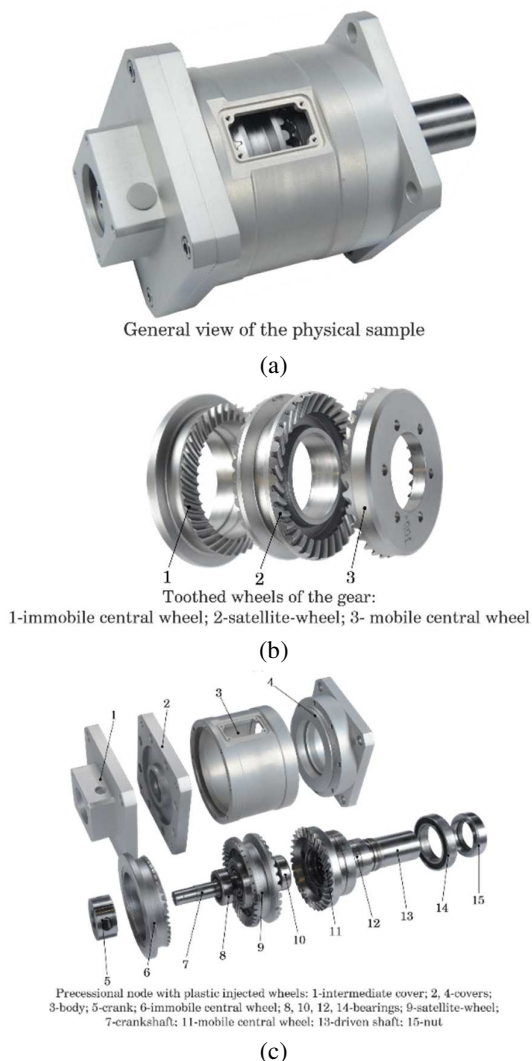


**Fig.14.** Sample of 2K-H ( $i = -75$ ) precessional transmission with gears  $A_{CX-CV}^{D, \beta}$

**8. CONCLUSIONS AND FINDINGS**  
*regarding the kinematic and functional possibilities of the precessional transmissions, the bearing capacity of the contact and the energy losses in the toothed gearings  $A_{CX-CV}^{D, \beta}$ :*

- The shape of the profile of the teeth of the central wheels has variable curvature, continuously increasing from the foot to the tip of the teeth, dependent on the configuration parameters  $[Z_g - \theta, \pm 1]$  and restricted by the condition of the basic principle of the fundamental law of gearing on ensuring the permanent constant ratio of

the motion transformation  $\omega_1/\omega_2=\text{const.}$  for any value of the precession angle  $\psi$ .

- The shape of the profile of the teeth of the central wheels with variable curvature, continuously increasing from the foot to the tip of the teeth is defined by the contact points  $k_i$  of the conjugated flanks of one and the same pair of teeth depending on the precession angle  $\psi$ .
- The number of pairs of teeth simultaneously conjugated at the same gearing phase, determined by  $\psi$ , is defined by the parametric configuration  $[Z_g - \theta, \pm 1]$  and by the size of the height of the teeth by cutting.
- The toothed precessional gear  $A^D$  with the correlation of the number of teeth  $Z_1=Z_2-1$  and  $Z_4=Z_3-1$  and the angle of the conical axoid  $\delta > 0^\circ$  is recommended for use in precessional transmissions with reducer operating regime, due to the geometry of the convex-concave contact  $K_{CX-CV}$  with the small difference in radii of curvature and the low relative sliding velocity between the conjugated flanks.
- The toothed precessional gear  $A^D$  with the correlation of the number of teeth  $Z_4=Z_3+1$  (or  $Z_1=Z_2+1$ ) and the angle of the conical axoid  $\delta \geq 0^\circ$  ensures the profile angle of the central wheel teeth greater than  $\alpha_w > 45^\circ$  and the operation of the transmission in multiplier mode, due to the favorable kinetostatics of transforming the rotational motion of the central wheel into spherospacial motion of the satellite wheel.
- In precessional gearing, the teeth contact on the portions of the active flanks, topologically dimensioned with the precession angle within the limits  $0^\circ \leq \psi \leq 180Z_2/Z_1$  and conjugate simultaneously in multiple pair contacts  $i$  with the dispersion determined by the relation  $\psi_{k_i} = 360Z_2i/Z_1^2$  which, as a whole, define the pressure angles  $\alpha_{w_i}$  between the flanks of the pairs of teeth conjugated simultaneously.

- Reducing dynamic loads and improving the lubrication conditions of the tooth flanks in the  $A_{CX-CV}^D$  gear can be achieved by creating cavities in the interdental space with functions of "pockets" of lubricant accumulation, including "cushions" for dynamic load damping, created as a result of the teeth tips profile of the satellite wheel with collateral circular arc with radius  $r_a > r$ .
- As a result of the spherospacial interaction of the multiple pair conjugated teeth from the precessional gear  $A_{CX-CV}^D$ , the linear contact between the flanks on the passive profiles migrates to the point  $k_0$ , thus ensuring the accumulation of lubricant in the interdental cavities and performing the function of "cushions" for damping dynamic loads.

**Acknowledgements:** The article was published by the authors by conducting scientific research under the State Research-Innovation Project, No. 160-PS of 31.01.2020 "Increasing the competitiveness of precessional transmissions by developing and capitalizing on the gear with conform contact of the teeth and expanding their application area". Project number 20.80009.700.24, dated 31.01.2020. Project leader - Acad. Ion Bostan.

### **Transmisii precesionale cu angrenări convex-concave multipare: sinteza structurală, cinematica și portanța contactului, generarea suprafețelor**

Articolul este dedicat cercetării transmisiilor precesionale (TP) cu angrenări convex-concave multipare ( $A_{CX-CV}^D$ ). Sunt abordate aspecte privind crearea angrenării precesionale cu contact convex-concav multipar al dinților, sinteza structurală a transmisiilor, cinematica și portanța contactului dinților. Se examinează influența parametrilor geometrici și cinematici ai angrenării convex-concave asupra alunecării relative cu frecare între flancurile conjugate ale dinților și asupra curburii reduse a profilurilor de flanc conjugate multipar și, respectiv, asupra capacității portante și a randamentului mecanic a angrenării. În lucrare sunt abordate procedee tehnologice de generare a profilurilor nestandarde ale dinților prin rulare cu sculă cu mișcare sferospațială, cât și prin generare în sistemul Gleason pe mașini-unelte cu comandă numerică. Sunt descrise aplicații constructiv-funcționale ale transmisiilor precesionale cinematice și de mică putere.

**Ion BOSTAN**, Academician, Doctor habilitates, University professor, Technical University of Moldova, L. Istrati str., 20, Chișinău, Republic of Moldova, [ion.bostan@cnts.utm.md](mailto:ion.bostan@cnts.utm.md)

## **9. REFERENCES**

- [1] Bostan, I. *Transmisii Precesionale: Sinteza, Cinematică și Elemente de calcul*. Vol. 1. Bons Offices, Chișinău, 2022. 517 p. ISBN 978-9975-87-978-1.
- [2] Bostan, I. *Transmisii Precesionale. Geometria, Cinematica și Portanța contactului*. Vol. 2. Bons Offices, Chișinău, 2022. 667 p. ISBN 978-9975-87-978-1.
- [3] Bostan, I. *Transmisii Precesionale. Generarea suprafețelor și Aplicații*. Vol. 3. Bons Offices, Chișinău, 2022. 589 p. ISBN 978-9975-87-981-1.
- [4] Bostan, I. A. *Precessionnye peredachi s mnogoparnym zacepleniem*. Știința, Chișinău, 1991. 356 p. ISBN 5-376-01005-08.
- [5] Bostan, V. *Modele matematice în inginerie*. Bons Offices, Chișinău, 2014. 470 p. ISBN 978-9975-80-831-6.
- [6] Wildhaber, E. *Helical gearing*. U.S. Patent nr. 1.601.750, 1926.
- [7] Novikov, M. L. *Zubchatye peredachi, a takzhe kulachkovye mexanizmy s tochechnoj sistemoj zacepleniya*. Avt. svid. SSSR no. 109113, 1956.
- [8] Bostan, I., Chisinau, MD; Bostan, V., Chisinau, MD; Vaculenco, M., Chisinau, MD; Deutsches Patent-und Markenamt; *Zahnradubertragung mit Prazessions bewegung*; DE 2120000799 U1 2022.11.03.